REGIONAL VELOCITY MODELS FOR GERMANY: A CONTRIBUTION TO THE SYSTEMATIC TRAVEL-TIME CALIBRATION OF THE INTERNATIONAL MONITORING SYSTEM

Jörg Schlittenhardt

Federal Institute for Geosciences and Natural Resources (BGR)
Stilleweg 2, 30655 Hannover, Germany

ABSTRACT

The purpose of this investigation was to derive a valid regional traveltime curve to improve seismic event location capability for strong events in Germany within the scope of calibration of the International Monitoring System (IMS) for the verification of the CTBT (Comprehensive Nuclear-Test-Ban Treaty). Onset times from the "Data Catalogues of Earthquakes in the Federal Republic of Germany and Adjacent Areas", published annually by BGR, for seismic phases from 1975–1995 were used to compute 4585 traveltimes for 958 earthquakes and explosions for the stations of the GRSN (German Regional Seismic Network). The advantage of this large data set over data from most active experiments is the unrivaled density and redundancy of the azimuthal coverage with raypaths across Germany. To assure the highest level of precision, only events with independently located epicenters from local networks have been included. The interpretation was carried out by trial-and-error modeling and linear regression of station traveltimes. Four traveltime branches (*Pn*, *Pg*, *Sn, Sg*) are clearly visible in the plot of station traveltimes as a function of distance, despite the large scatter (standard deviation over 2 s for *P* and 3 s for *S*). Other branches, such as *P** (Conrad refracted wave), are not visible. The model obtained by inversion has one layer over a half space. *P*- and *S*-velocities for the layer are 5.9 km/s and 3.5 km/s, respectively. The inferred layer thickness is 30 km, in accordance with the poorly determinable values of intercept time and crossover distance. The sub-Moho *P*- and *S*-velocities are 8.2 km/s and 4.73 km/s, respectively. Tests of the location capability for selected ground truth events (explosions for refraction seismic experiments) in Germany and Poland are presented. The application of the new model distinctly reduces traveltime residuals for the routine determination of epicenters.

Besides inaccurate epicenter parameter values, an azimuthally dependent *Pn* velocity can possibly explain the large scatter of the traveltimes. Due to the abundance of available raypaths, this data set offers a unique opportunity to test models of mantle anisotropy in Central Europe. Subsets are formed of traveltimes for selected pairs of an epicenter and a station in azimuth slices covering all directions. Typically, about 600 raypaths fall into a slice of 30º width. Directions with postulated fast (N30ºE) and slow (N120ºE) sub-Moho velocities found in controlled source experiments (e.g., Enderle et al., 1996) are examined. Although there is a trade-off between source depth and *Pn* velocity, a clear advance of *Pn* arrivals is observed for the fast direction, compared to the traveltimes for the best-fit model. Further results of the *Pn* velocity mapping for different azimuth slices for the region between the Alpine Front in the south and 52ºN will be presented. The study is supplemented with seismic record sections for selected azimuth directions for the magnitude Ml=4.8 rockburst at Teutschenthal near Halle, Germany ("ground truth" event), which was recorded by a number of permanent (GRF/GRSN, GERESS, GOR, LED, SED, etc.) and portable TOR (Teleseismic Tomography TORnquist experiment) digital stations in Germany and adjacent areas.

Key Words: Seismic wave propagation, regional phases, crustal structure, seismic anisotropy, seismic regionalization, IMS, earthquake location, ground truth

OBJECTIVE

The initial motivation for this study came from the GSETT-3 (Group of Scientific Experts Technical Test) experiment of the CD (Conference on Disarmament) in Geneva, where NDC's (National Data Center) were asked to check the location results of the pIDC (prototype International Data Center) for seismic events on their national territory.
The primary objective of this investigation is therefore to derive a valid regional traveltime curve on a large scale to improve seismic event location capability for strong events in Germany within the scope of calibration of the International Monitoring System (IMS) for the verification of the CTBT (Comprehensive Nuclear-Test-Ban Treaty). The derived traveltime curve is intended to be used rather with data from a sparse global network (stations several hundreds of kilometers apart) instead of with data from dense local networks (station spacing tens of kilometers, or less), for which specific models would be needed.

RESEARCH ACCOMPLISHED

The data used in this study stem from the "Data Catalogues of Earthquakes in the Federal Republic of Germany and Adjacent Areas", published annually by BGR (Bundesanstalt für Geowissenschaften und Rohstoffe, (Henger & Leydecker (eds.), 1975)). From this catalogue, onset times for seismic phases from 1975–1995 were used to compute 4585 traveltimes for 958 earthquakes and explosions for the stations of the GRSN (German Regional Seismic Network). To assure the highest level of precision, only events with independently located epicenters from local networks within Germany (University institutes and State Geological Surveys) have been included. The interpretation is carried out by trial-and-error modeling and linear regression of station traveltimes.

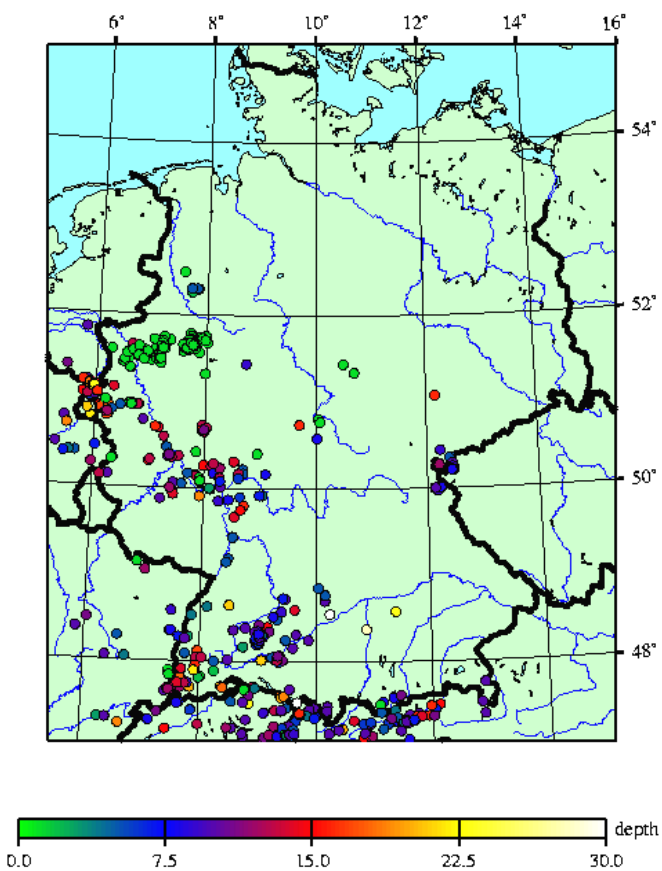

Fig. 1: Map of Germany with the plot of the epicenters of the 958 earthquakes/explosions used in this study. Hypocentral depth is color coded according to the depth scale (km) at the bottom. The seismicity follows essentially the Alpine belt in the south and the north-south trending Rhine Graben. The Swabian

Alb (in the southwest) and the Vogtland area also contribute to the seismicity. Fig. 2 shows a map with a plot of the ray paths from the 958 epicenters to the stations of the GRSN and their predecessor stations.

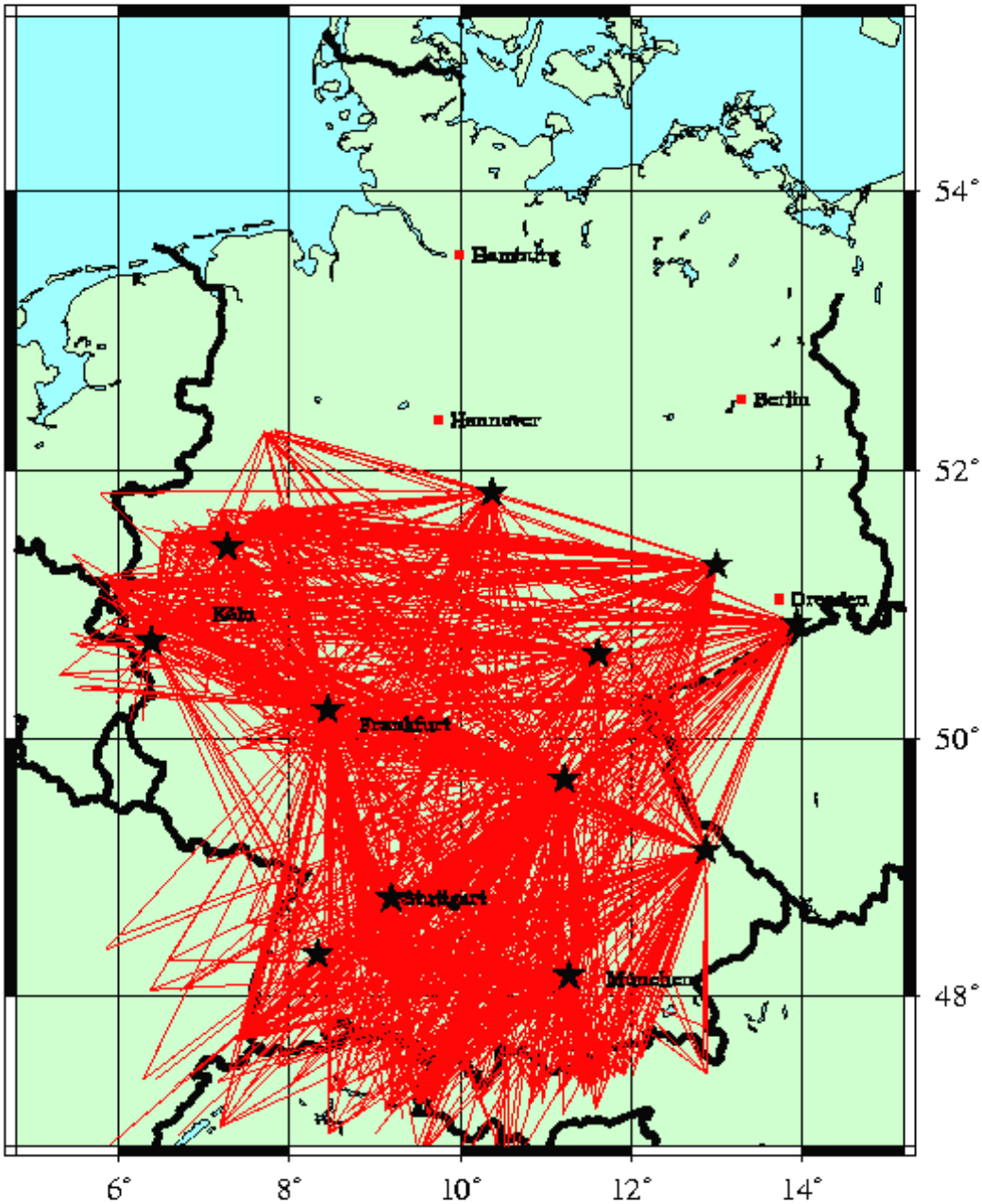

Fig. 2: Map of Germany with the plot of the ray paths (surface projection) from the 958 epicenters to the stations of the GRSN (stars).

The coverage with ray paths south of latitude 52° N in the center and the southern part of Germany is rather well. The north is not covered. The advantage of this large data set over data from most active experiments is the unrivaled density and redundancy of the azimuthal coverage with raypaths across Germany. This is demonstrated in Fig. 3, which shows a uniform distribution of distance and azimuth.

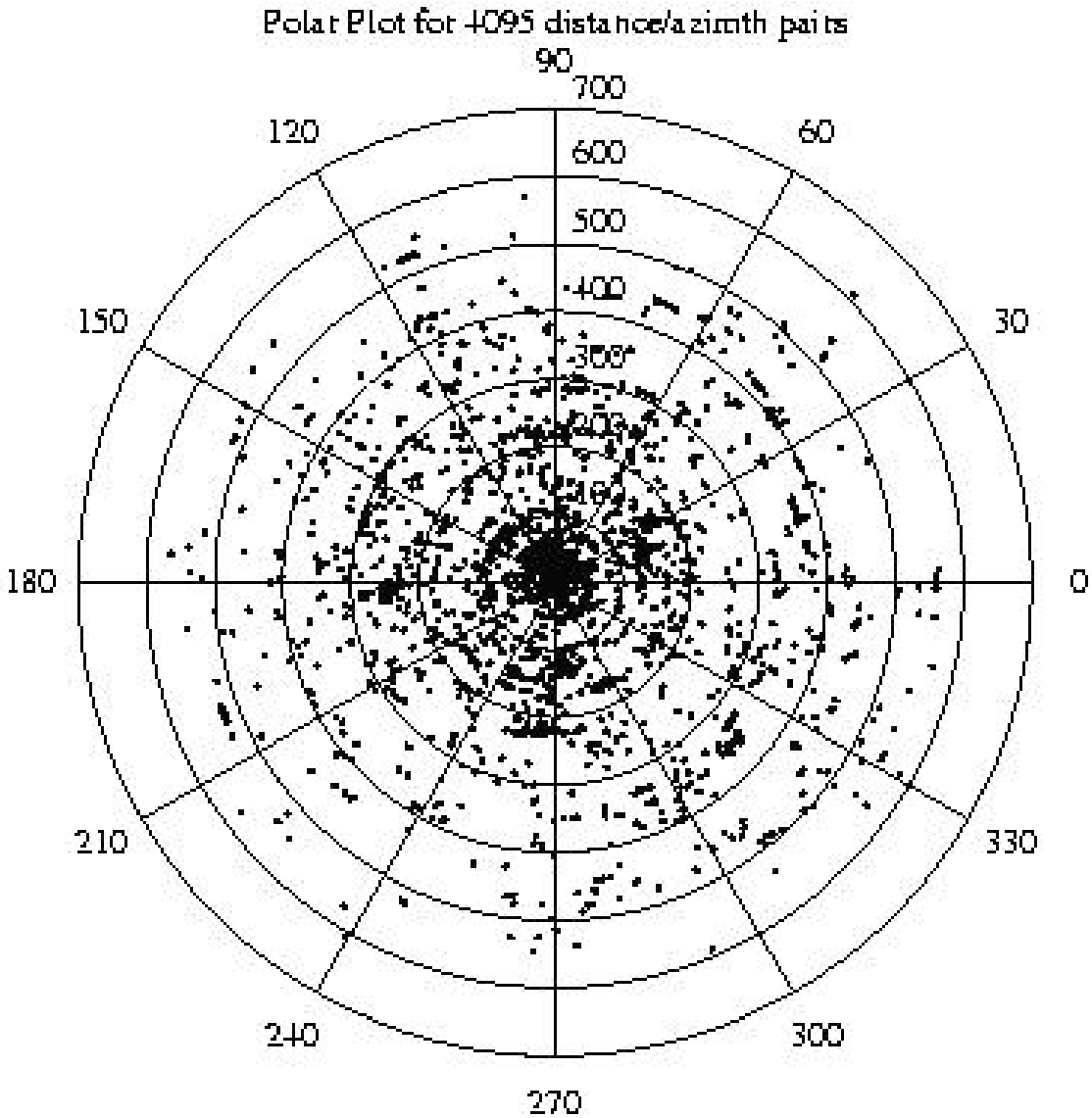

Fig. 3: Polar plot for 4095 distance-azimuth pairs used in this study. Note that azimuth is plotted counter clock wise from north (right). Labels on the concentric circles give distance in kilometers.

Fig. 4 shows a representation of the 4585 station traveltimes as function of epicenter distance. Four traveltime branches (*Pn*, *Pg*, *Sn, Sg*) are clearly visible, despite the large scatter (standard deviation over 2 s for *P* and 3 s for *S*). Other branches, such as *P** (Conrad refracted wave), are not visible.

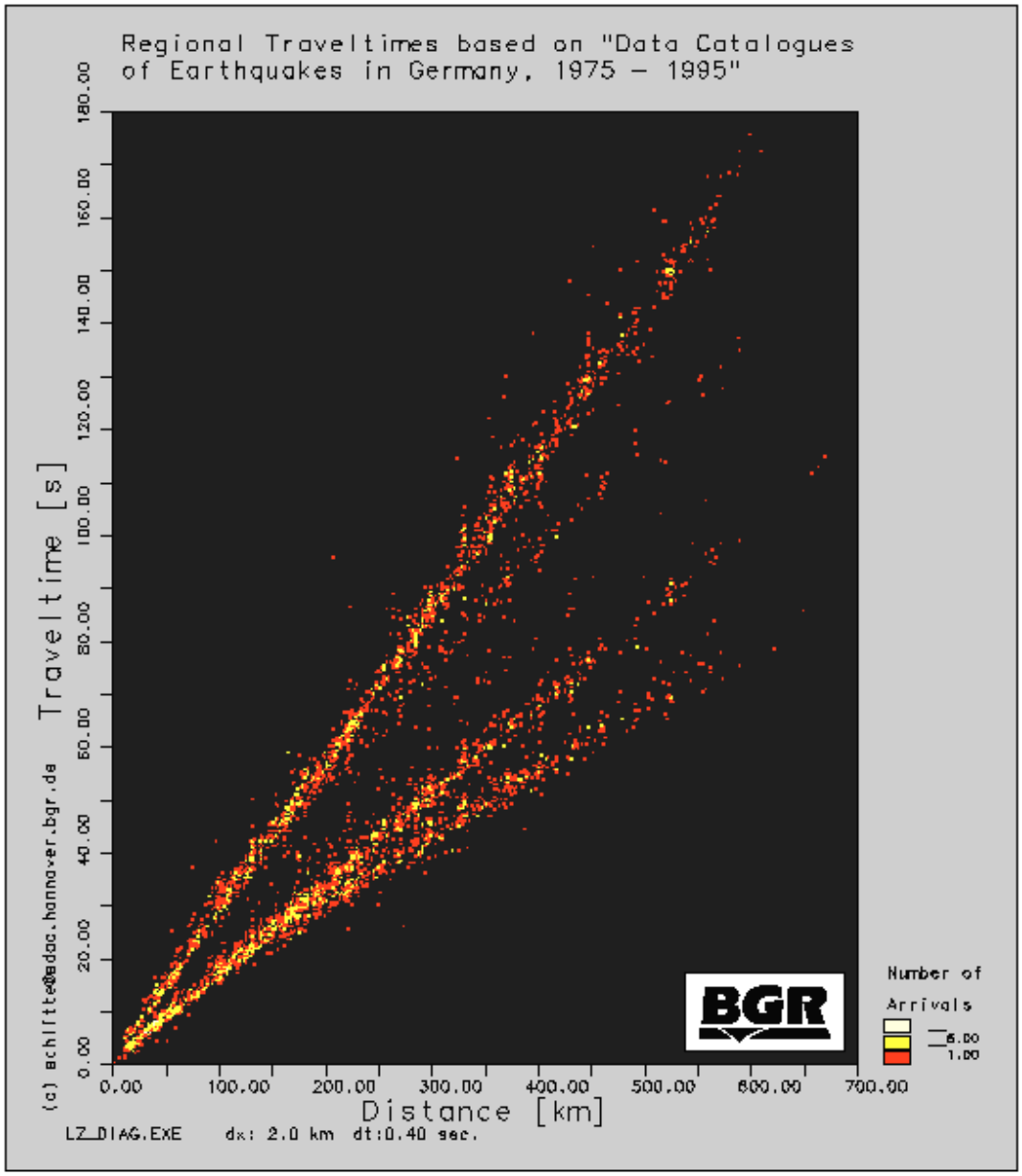

Fig. 4: Representation of the 4585 station traveltimes as a function of epicenter distance. For the plot, the number of arrivals in each bin with a width of *dx*=2 km and *dt*=0.4 s is counted and color-coded according to the scale at the right.

Taking into account the large scatter of the data, at first, an adequate interpretation of the traveltimes is achieved by a simple model with one layer over a half space. The interpretation was made interactively graphical as well as by linear regression of station traveltimes. Fig. 5 shows the data from the previous Fig. 4 with reduced traveltimes.

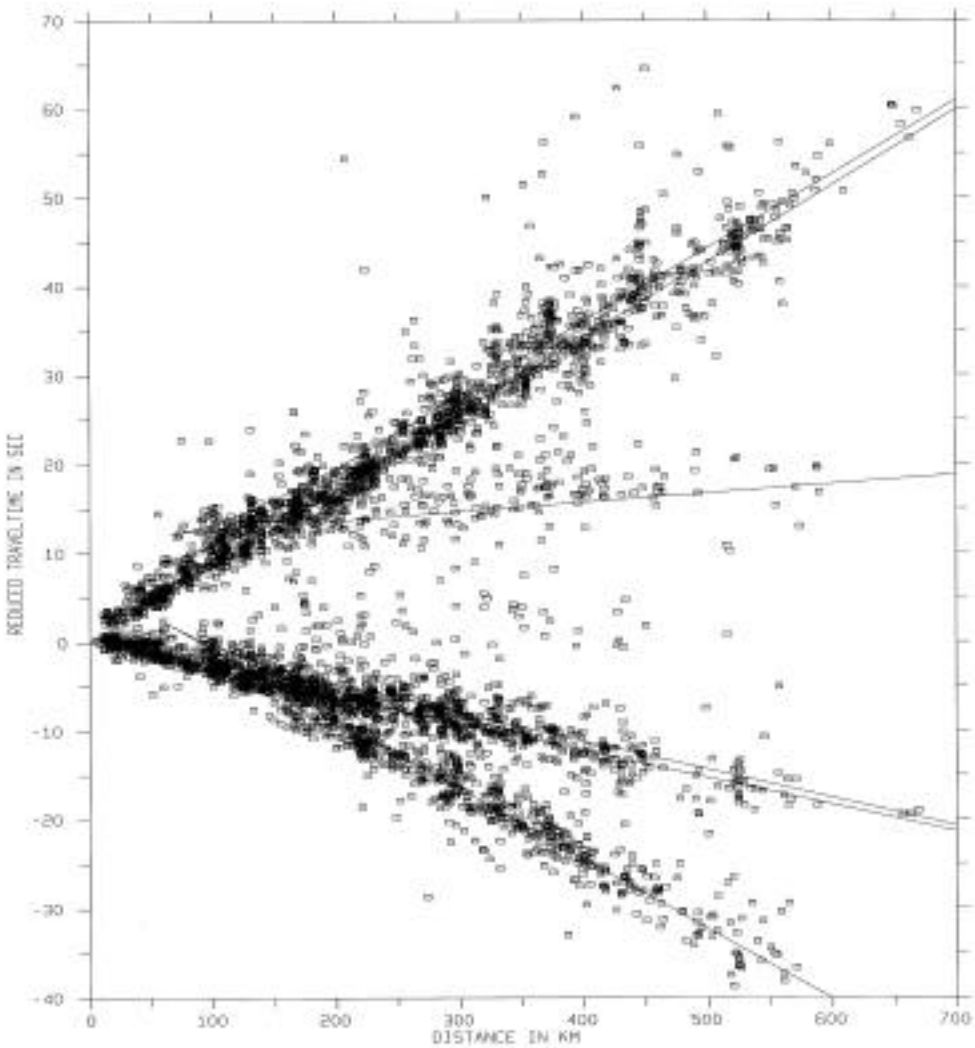

Fig. 5: Reduced traveltime plot of the data from Fig. 4. The reduction velocity (5 km/s) is used to help separate *P*- and *S*-wave traveltime branches. The superimposed theoretical traveltime curves for *Pn*, *Pg*, *PmP, Sn, SmS* and *Sg* stem from the best fitting model.

The reduction velocity of 5 km/s is used to help separate *P*- and *S*-wave traveltime branches. In this representation *P*-wave branches have negative slope, *S*-wave traveltime branches have positive slope. The superimposed theoretical traveltime curves for P_n, P_g, *PmP* and S_n, S_g, *SmS* stem from the best fitting model, which was found by trial-and-error modeling of vertically inhomogeneous velocity depth distributions. The model obtained by inversion has one layer over a half space. *P*- and *S*-velocities for the layer are 5.9 km/s and 3.5 km/s, respectively. The inferred layer thickness is 30 km, in accordance with the poorly determinable values of intercept time and crossover distance. The sub-Moho *P*- and *S*-velocities are 8.2 km/s and 4.73 km/s, respectively. Besides this graphical fitting of the traveltime curves a linear regression of the station traveltimes was made using two approaches. Table 1 shows the apparent velocities of the four main crustal phases as determined by 'using the phase code' and by 'ignoring the phase code', respectively, given in the earthquake catalogue. The apparent velocities for a given phase inferred

Table 1: Apparent velocities and confidence limits (2 σ-level) for the phases Pn, Pg, Sn and Sg as determined by linear regression using two approaches. The results of the trial-and-error modeling are given in the first column in brackets for comparison.

	Using Phase Code		Ignoring Phase Code	
Phase	Velocity (km/s)	2 σ s)	Velocity (km/s)	2 σ (s)
Pn (8.2)	8.04	6.56	8.52	4.20
Pg (5.9)	6.12	(4.21	6.02	1.71
Sg (3.5)	3.51	5.91	3.57	3.86
Sn (4.73)	4.74	8.57	4.93	5.80

from linear regression differ strongly. This result reflects the difficulties encountered selecting appropriate distance-traveltime sections for the regression. The conclusion is to give the trial-and-error modeling results priority over the only apparently more objective regression results.
Fig. 6 shows a comparison of the model derived here with a similarly simple model, namely the IASPEI91 model

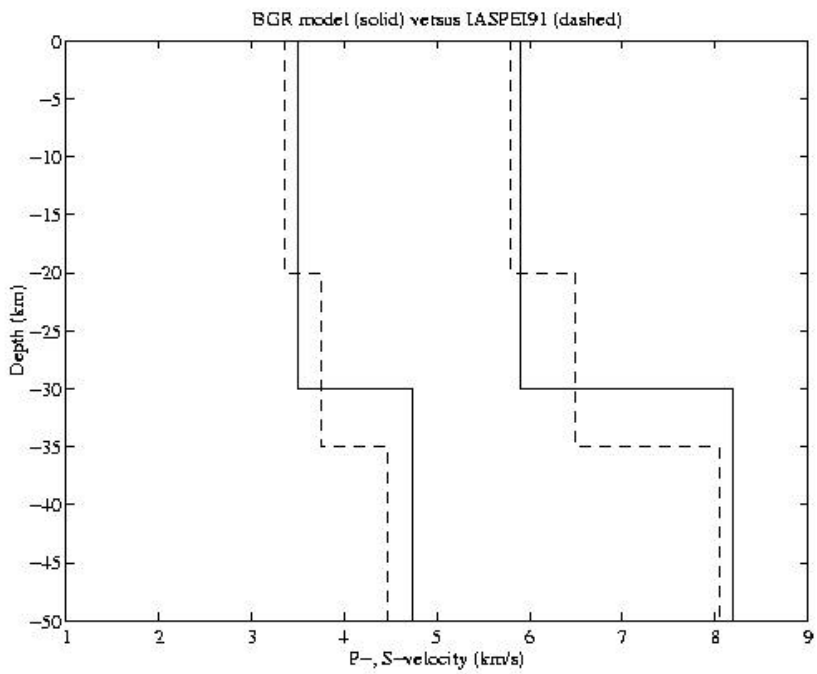

Fig. 6: Comparison of the model derived in this study (solid) with the IASPEI91 model (dashed) used at the IDC. For both models the *P*- and *S*-velocities, respectively, are given.

used at the IDC. Because of the different *Pn* and *Sn*, but also because of the different *Pg* and *Sg* velocities, considerable location differences result. Fig. 7 shows the *Sn-Pn* difference traveltimes for the two models of the previous

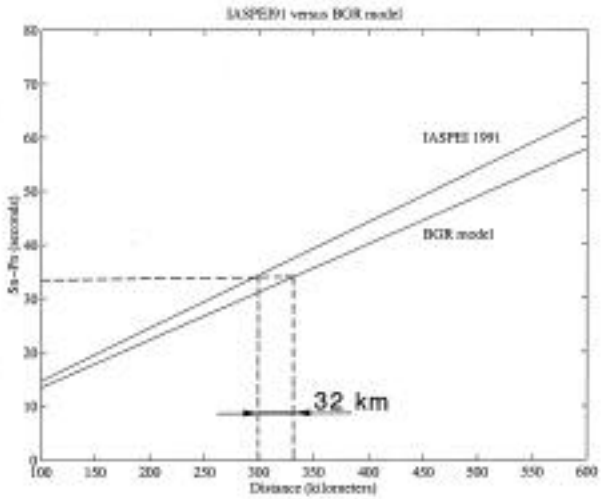

Fig. 7: *Sn-Pn* difference traveltimes for the IASPEI91 and BGR model (see labels**).**

Fig. 6. When using solely *Sn-Pn* difference travel times, for theses two models differences in localization of over 30 km result for observation distances of around 300 km. However, the best possibility to check the reliability of localization procedures and the underlying velocity models is to use so called 'ground truth' events as a reference. Such events are often not easily found. I use here the underground explosions of the seismic experiments GRANU95 and POLONAISE97 as well as the rockburst near Halle, Germany, of September 1996 as ground truth. Stars in Fig. 8 show the location of these events.

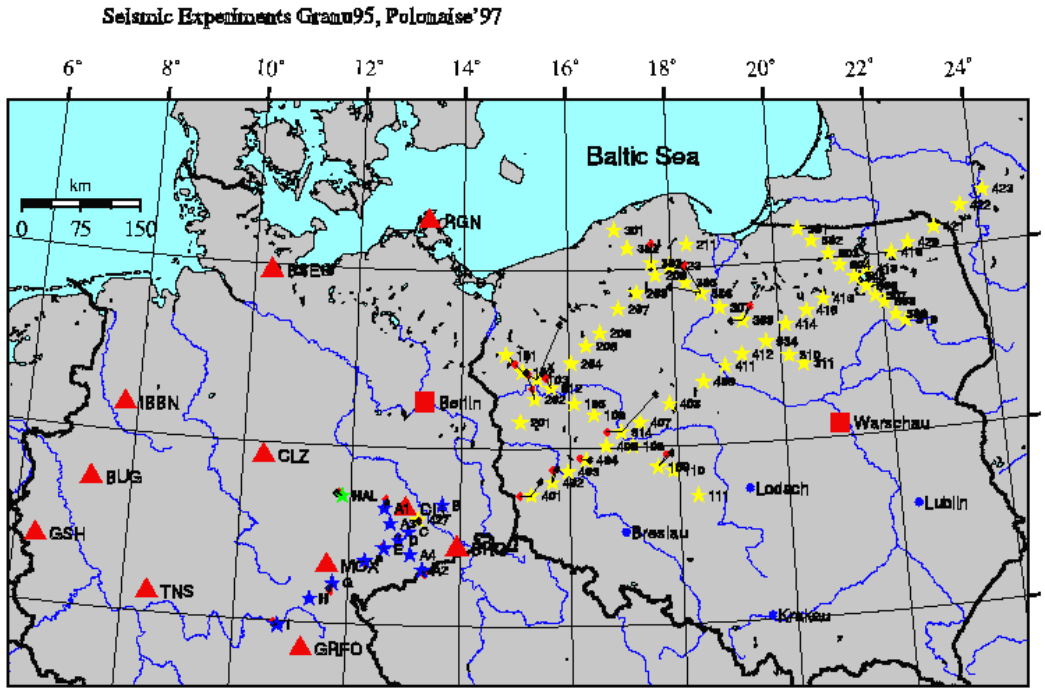

Fig. 8: Shot locations of the seismic experiments GRANU95 (dark stars) and POLONAISE97 (bright stars) in Germany and Poland, respectively. The location of the rockburst at Teutschenthal near Halle (Germany) is marked by a star labeled HAL. Triangles show the locations of GRSN stations**.**
The charge sizes used for these explosions reached from below hundred to thousand kilogram, the corresponding M_L values were in the range 0.5 - ~ 3.0. Fig. 9 shows a detail map of the region shown in Fig. 8

with the seismic localization results for the GRANU95 shots, the rockburst at Teutschenthal near Halle (Germany) and shot '427' of the POLONAISE97 seismic experiment.

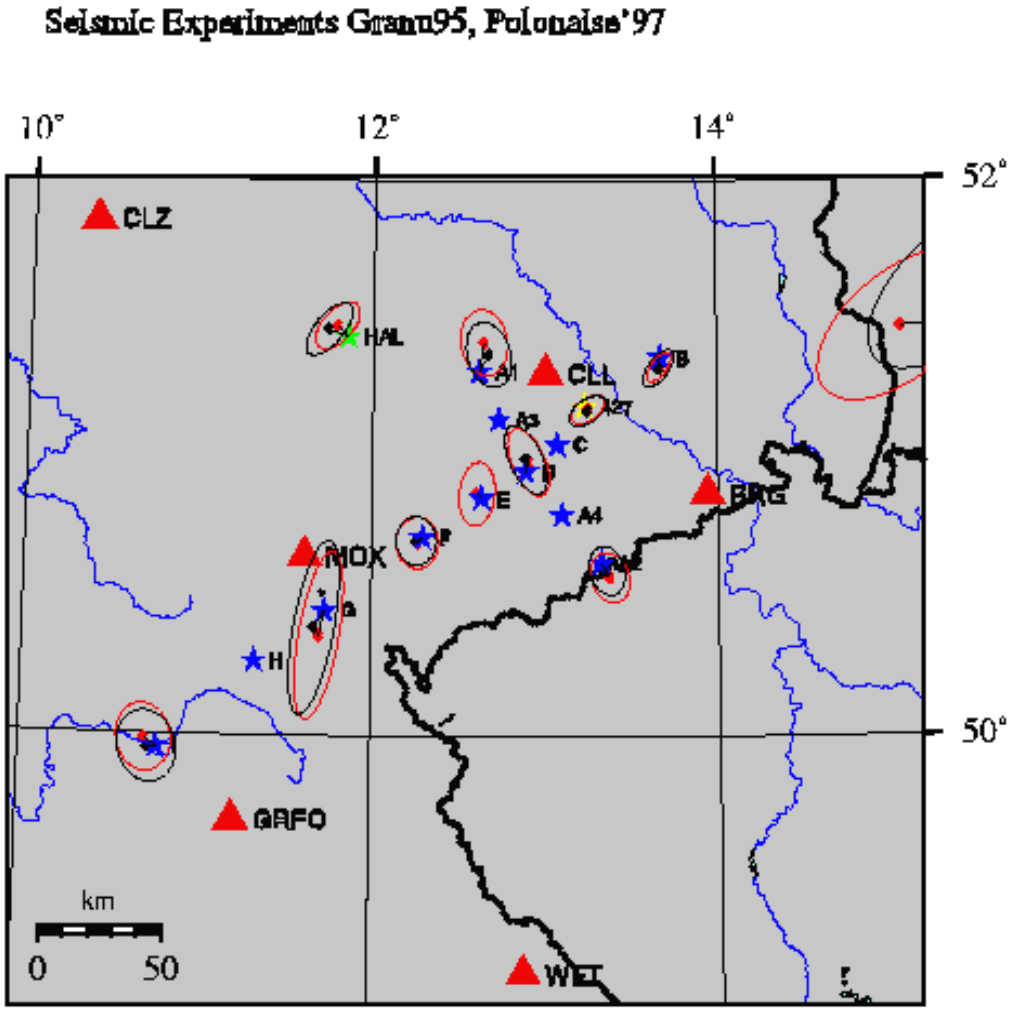

Fig. 9: Detail map of the border region Germany – Czech Republic – Poland showing the seismic localization results for the GRANU95 shots, the rockburst at Teutschenthal near Halle (Germany) and shot '427' of the POLONAISE97 seismic experiment. The dots and ellipses (BGR red; IASPEI91 black) give the locations and error ellipses determined using the two different models. Stars give 'Ground truth' locations. Triangles show the locations of GRSN stations**.**

Red and black dots and ellipses mark the locations determined using the BGR and IASPEI91 model, respectively. There is generally good agreement between the seismically determined locations (dots) and the 'ground truth' locations. With the exception of GRANU95 shot 'I', for all other explosions only *Pg*-phases of the stations BRG, CLL and MOX could be used. The good agreement between the localization results for the two models can be explained by the fact that the *Pg* velocities of the IASPEI91 and BGR model are only slightly different. Shot 'G', which is located outside the three-station subnet BRG, CLL and MOX, clearly shows the largest error ellipse. Fig. 10 shows a detail map of the western part of Poland with the seismic localization results of selected POLONAISE97 shots.

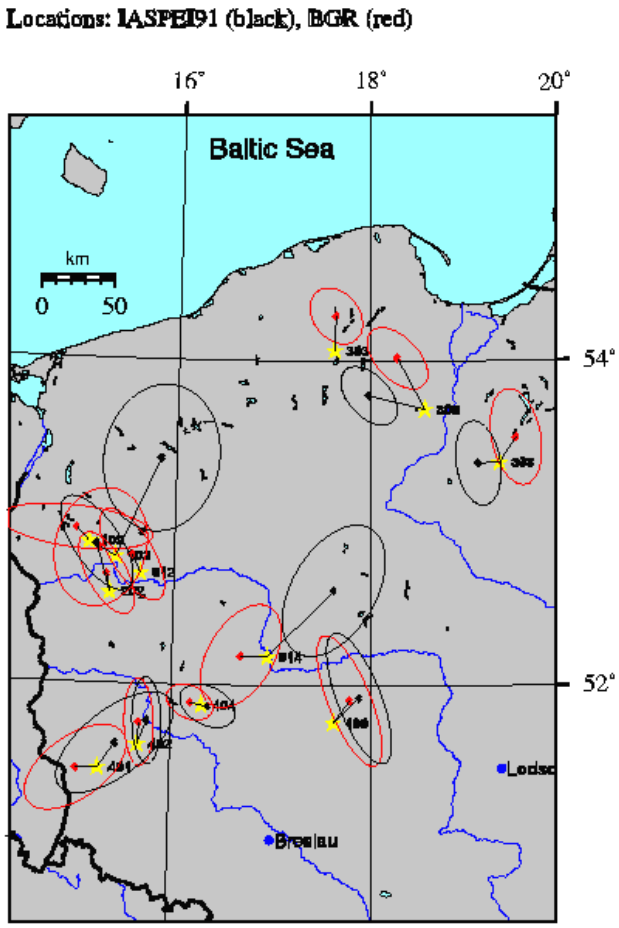

Fig. 10: Detail map of the western part of Poland with the border to Germany at the left showing the seismic localization results for selected POLONAISE97 explosions. The dots and ellipses (BGR red; IASPEI91 black) give the locations and error ellipses determined using the two different models. Stars give 'Ground truth' locations. Note that for some of the explosions (e.g. shot '303') no location was found using the IASPEI91 model.

These examples represent the borderline case were all seismic events are located outside the recording regional network. For the majority of the explosions close to the German border the localizations using the BGR model lie closer to the 'ground truth' locations. For some of the more distant explosions there is no convergence of the Geiger method when the IASPEI91 model is used.

CONCLUSIONS AND RECOMMENDATIONS

The model obtained in this study by inversion of earthquake/explosion bulletin data ("Data Catalogues of Earthquakes in the Federal Republic of Germany and Adjacent Areas") has one layer over a half space. *P*- and *S*-velocities for the layer are 5.9 km/s and 3.5 km/s, respectively. The inferred layer thickness is 30 km, in accordance with the poorly determinable values of intercept time and crossover distance. The sub-Moho *P*- and *S*-velocities are 8.2 km/s and 4.73 km/s, respectively. Tests of the location capability for selected ground truth events (explosions for refraction seismic experiments) in Germany and Poland are presented which confirm the validity of the model. The application of the new model distinctly reduces traveltime residuals for the routine determination of epicenters.
Besides inaccurate epicenter parameter values, an azimuthally dependent *Pn* velocity can possibly explain the large scatter of the observed traveltimes. Due to the abundance of available raypaths, this data set offers a unique opportunity to test models of mantle anisotropy in Central Europe. Subsets are formed of

traveltimes for selected pairs of an epicenter and a station in azimuth slices covering all directions. The results are presented in Fig. 11.

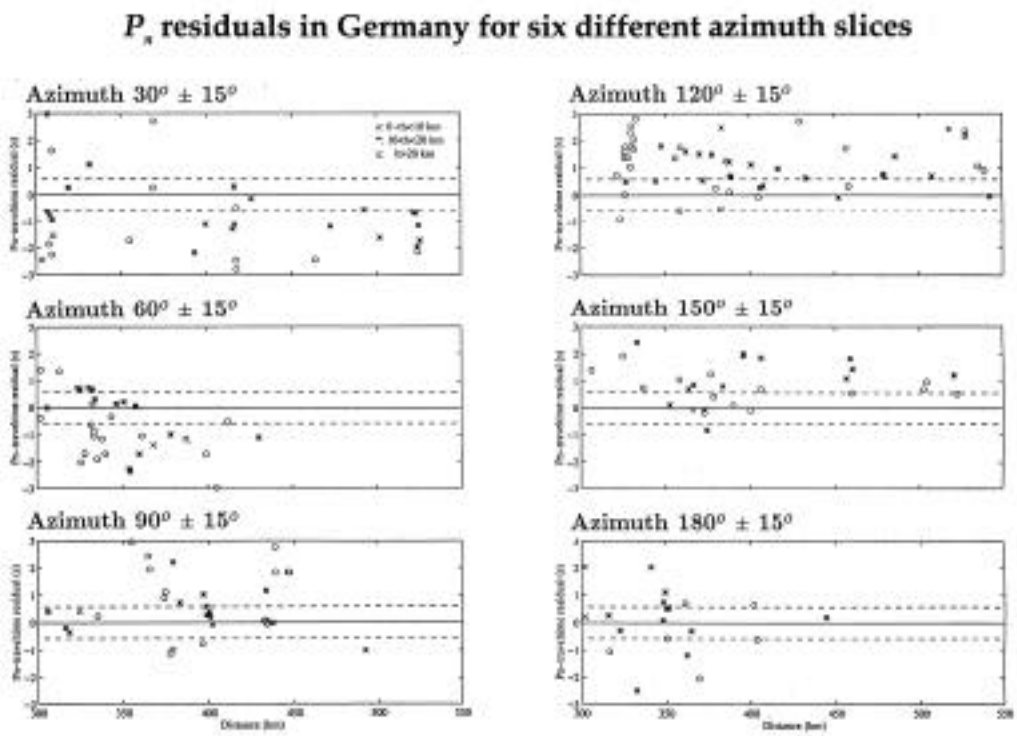

Fig. 11: *Pn* residuals for six different azimuth slices of 30º width (see labels) as a function of distance. The hypocenters of the earthquakes used are from depths *h* within three consecutive intervals of 10 km thickness (symbols in sub-plot top, left). The heavy lines and the two dashed lines correspond to the theoretical residuals for the middle and the top and bottom of the three depth intervals (5±5km, 15±5km, 25±5km), respectively. There exists an azimuth dependence of the residuals, particularly for the postulated fast (30º±15º) and slow (120º±15º)) directions**.**

Typically, about 600 raypaths fall into a slice of 30º width. Directions with postulated fast (N30ºE) and slow (N120ºE) sub-Moho velocities found in controlled source experiments (Prodehl & Giese, 1990; Enderle et al., 1996) can be confirmed (see residuals for the corresponding azimuth in Fig. 11). Although there is a trade-off between source depth and *Pn* velocity, a clear advance of *Pn* arrivals is observed for the fast direction, compared to the traveltimes for the best-fit model. It is recommend to use the unique data set presented in this study for future investigations of anisotropy and 3-D velocity structure (tomography) to further improve localization capabilities.

REFERENCES

Henger, M., Leydecker, G., (Eds.), 1975 (and following years). Data catalogue of earthquakes in the Federal Republic of Germany and adjacent areas, *Data of the Seismological Observatories in the Federal Republic of Germany compiled and edited by the Bundesanstalt für Geowissenschaften und Rohstoffe, Hannover*, Hannover.

Enderle, U., Mechie, J., Sobolev, S., Fuchs, K., (1996). Seismic anisotropy within the uppermost mantle of southern Germany. *Geophys. J. Int.*, **125**, 747-767

Prodehl, C., P. Giese, 1990. Seismic investigations around the EGT in Central Europe, in *The European Geotraverse: integrative studies - results from the 5th Earth Science Study Centre*, R.Freeman, P.Giese, St.Mueller (ed.), 77-97, European Science Foundation, Straßburg.